Theoretical Studies of the Absorption and Emission Properties of the Fluorene-Based Conjugated Polymers

7 AUTHORS, INCLUDING:

Ji-fen Wang

Shanghai Second Polytechnic University

29 PUBLICATIONS **456** CITATIONS

SEE PROFILE

Ai-Min Ren

Jilin University

248 PUBLICATIONS **2,344** CITATIONS

SEE PROFILE

Ping Lu

Zhejiang University

334 PUBLICATIONS **6,868** CITATIONS

SEE PROFILE

Theoretical Studies of the Absorption and Emission Properties of the Fluorene-Based Conjugated Polymers

Ji-Fen Wang,[†] Ji-Kang Feng,*,[†,‡] Ai-Min Ren,[†] Xiao-Dong Liu,[†,‡] Yu-Guang Ma,[§] Ping Lu,[§] and Hong-Xing Zhang[†]

State Key Laboratory of Theoretical and Computational Chemistry, Institute of Theoretical Chemistry, Jilin University, Changchun 130023, P.R. China; College of Chemistry, Jilin University, Changchun 130023, P.R. China; and Key Laboratory for Supramolecular Structure and Materials of Ministry of Education, Institute of Theoretical Chemistry, Jilin University, Changchun 130023, P.R. China

ABSTRACT: The structures, ionization potentials (IPs), electron affinities (EAs), and HOMO−LUMO gaps (Δ_{H-L}) of the oligomers are studied by the density functional theory with B3LYP functional. The lowest excitation energies (E_gs) and the maximal absorption wavelength λ_{abs} of oligomers of polyfluorene (PF) and poly(2,7-fluorene-*alt-co*-5,7-dihydrodibenz[*c,e*]oxepin) (PFDBO) are studied employing the time-dependent density functional theory (TD-DFT) and ZINDO. Band gaps and effective conjugation lengths of the corresponding polymers were obtained by extrapolating HOMO−LUMO gaps and the lowest excitation energies to infinite chain length. The IPs, EAs, and λ_{abs} of the polymers were also obtained by extrapolating those of the oligomers to the inverse chain length equal to zero ($1/n = 0$). For PFDBO, IPs and EAs are higher and the band gap is larger than those of PF's from the extrapolation. The outcome shows that the dramatically twisted structure of PFDBO in the seven-membered ring results in the decreased conjugation in the chain. These cause both the maximal absorption and emission wavelengths of PFDBO blue shift compared with PF.

1. Introduction

Theoretical studies on the electronic structures of polymers have contributed a lot to rationalize the properties of known polymers[1−8] and to predict those of yet unknown ones.[9−11] There are two different theoretical approaches to evaluate the band gaps of polymers. One is the polymer approach in which the periodic structures are assumed for infinite polymers.[12−14] Another one, the oligomer extrapolation technique,[6,15,16] has acquired the increasing popularity in this field, however. In this approach, a sequence of increasing longer oligomers is calculated, and extrapolation to infinite chain length is followed.[6,17] A distinct advantage of this approach is that it can provide the convergence behavior of the structural, electronic, and spectral properties of polymers.[18] In practice, both the oligomer extrapolation and the polymer approaches are generally considered to be complementary to each other in understanding of the properties of polymers. Obviously, a theoretical investigation on the band gaps of these polymers is very instrumental in guiding the experimental synthesis,[19,20] which is the topic of the present work. Here we studied two fluorene-based copolymers polyfluorene (PF) and poly(2,7-fluorene-*alt-co*-5,7-dihydrodibenz[*c,e*]oxepin) (PFDBO) (shown in Figure 1) using density functional methods and semiclassical models. Energy gap is the orbital energy difference between the highest occupied molecular orbital (HOMO) and the lowest unoccupied molecular orbital (LUMO), which is band gap in polymer. We can obtain the correct
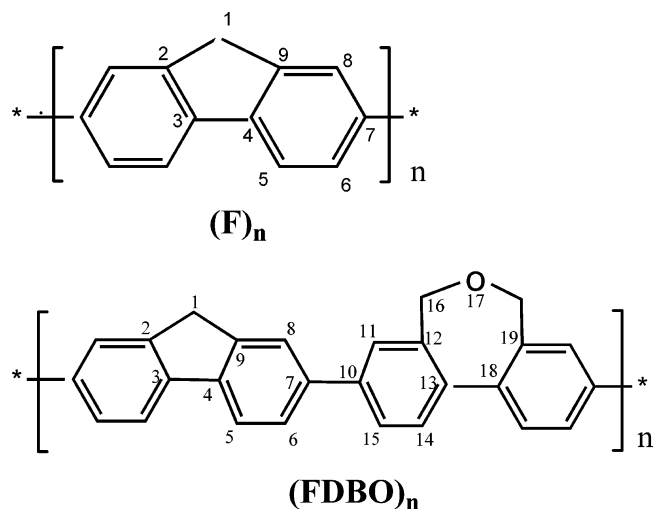
Figure 1. Sketch map of the structures.

values of the energy gap from the proper theoretical method. However, the accurate orbital energy cannot be easily obtained by experiment. The experimental band gap is generally estimated from the cyclic voltammograms (CV) and onset wavelength of the optical absorption from ultraviolet light (UV).[21] Different from other investigations, the main feature of this work is extrapolating the resultant linear relationship to infinite chain length to obtain the IPs and EAs of the polymers as well as energy gaps and absorption wavelengths.

2. Computational Details

The ground-state geometries of oligomers were fully optimized using the density functional theory (DFT), B3LYP/6-31G, as implemented in Gaussian 03. ZINDO and TD-DFT/B3LYP calculations of the lowest excitation energies and the maximal absorption wavelengths

[†] State Key Laboratory of Theoretical and Computational Chemistry, Institute of Theoretical Chemistry.
[‡] College of Chemistry.
[§] Key Laboratory for Supramolecular Structure and Materials of Ministry of Education, Institute of Theoretical Chemistry.
* Corresponding author: e-mail jikangf@yahoo.com; FAX +86-431-8945942.

Table 1. Optimized Geometry Parameters of (FDBO)$_n$ and (F)$_n$ ($n = 1-4, 6, 8$) Bond Lengths (10^{-10} m) and Angles (deg)

| n	(FDBO)$_n$				(F)$_n$					
	1	2	3	4	1	2	3	4	6	8
$r(1,2)$	1.521	1.522	1.521	1.521	1.520	1.521	1.521	1.521	1.521	1.521
$r(3,4)$	1.470	1.462	1.468	1.468	1.472	1.470	1.468	1.468	1.468	1.468
$r(4,5)$	1.398	1.403	1.399	1.399	1.399	1.398	1.399	1.399	1.399	1.399
$r(5,6)$	1.397	1.393	1.397	1.397	1.400	1.397	1.397	1.397	1.397	1.397
$r(6,7)$	1.412	1.422	1.412	1.412	1.403	1.412	1.412	1.413	1.413	1.413
$r(7,8)$	1.413	1.426	1.413	1.413	1.404	1.413	1.414	1.414	1.414	1.414
$r(8,9)$	1.389	1.383	1.389	1.389	1.393	1.389	1.389	1.389	1.389	1.389
$r(4,9)$	1.416	1.425	1.416	1.417	1.416	1.416	1.416	1.417	1.416	1.417
$r(7,10)$	1.485	1.467	1.485	1.485						
$r(10,11)$	1.408	1.419	1.408	1.408						
$r(11,12)$	1.399	1.393	1.399	1.399						
$r(12,13)$	1.418	1.430	1.419	1.419						
$r(13,14)$	1.407	1.417	1.407	1.407						
$r(14,15)$	1.394	1.387	1.394	1.394						
$r(15,10)$	1.409	1.421	1.409	1.409						
$r(13,18)$	1.486	1.466	1.484	1.484						
$r(12,16)$	1.512	1.511	1.512	1.512						
$r(16,17)$	1.467	1.468	1.466	1.467						
$\theta(1,2,3)$	110.02	109.47	109.97	109.98	110.04	110.03	109.95	109.95	109.95	109.94
$\theta(2,3,4)$	108.56	109.10	108.69	108.67	108.60	108.55	108.70	108.69	108.69	108.70
$\theta(2,1,9)$	102.72	102.85	102.69	102.69	102.74	102.73	102.71	102.71	102.71	102.71
$\theta(9,4,5)$	119.88	118.81	119.89	119.88	120.37	119.82	119.83	119.83	119.82	119.85
$\theta(4,5,6)$	119.19	119.65	119.18	119.18	118.93	119.21	119.19	119.19	119.20	119.18
$\theta(5,6,7)$	121.56	122.37	121.57	121.56	120.65	121.63	121.65	121.65	121.66	121.63
$\theta(8,7,10)$	120.62	121.39	120.62	120.55						
$\theta(10,11,12)$	122.10	122.94	122.11	122.09						
$\theta(11,12,13)$	119.65	120.23	119.65	119.65						
$\theta(12,13,14)$	118.39	117.00	118.36	118.37						
$\theta(12,13,18)$	120.62	121.59	120.59	120.63						
$\theta(16,12,13)$	119.95	119.72	119.96	119.96						
$\theta(17,16,12)$	114.77	115.72	114.82	114.86						
$\Phi(1,2,3,4)$	0.045	0.279	0.257	0.406	0.00	0.042	0.289	0.316	0.403	0.399
$\Phi(2,3,4,9)$	0.142	0.361	0.301	0.391	0.00	0.191	0.359	0.025	0.134	0.099
$\Phi(4,5,6,7)$	0.086	0.030	0.071	0.022	0.00	0.012	0.093	0.118	0.178	0.154
$\Phi(8,7,10,15)$	35.97	35.89	36.01	36.33		36.62	36.42	37.67	37.17	37.00
$\Phi(10,15,14,13)$	0.116	0.146	0.146	0.145						
$\Phi(12,13,18,19)$	42.65	41.95	41.92	42.03						
$\Phi(16,12,13,18)$	3.77	4.30	3.91	3.98						
$\Phi(17,16,12,13)$	72.57	72.78	72.67	72.54						

(λ_{abs}) were then performed at the optimized geometries of the ground states. The excited geometries were optimized by ab initio CIS/3-21G, and the emission spectra were computed on the basis of the excited geometries. All of IPs and EAs involved in this paper are the energies' difference between the ions and molecules. We employed the linear extrapolation technique in this research.[22] The linearity between the calculated IPs, EAs, energy gap, maximal absorption wavelengths of the oligomers, and the reciprocal chain length is excellent for both homologous series of oligomers. Thus, these values of the polymers can be obtained by extrapolating the resultant linear relationship to infinite chain length. In addition, the effective conjugation length (ECL) was estimated by the convergence of the excitation energies with the chain length within a threshold of 0.01 eV, based on the obtained linearity between the excitation energy and reciprocal chain length.

3. Results and Discussion

Ground Structural Properties. The oligomers' structural properties of (F)$_n$ and (FDBO)$_n$ from calculations by (DFT)B3LYP/6-31G are given below.

The results of the optimized structures for the oligomeric molecules of the (F)$_n$ ($n = 1-4, 6, 8$) and (FDBO)$_n$ ($n = 1-4$) show that the structural changes softly with increasing chain length in the series of (F)$_n$ as well as (FDBO)$_n$, except the (F)$_3$ has a larger dihedral 0.36° in the five-membered ring $\Phi(2,3,4,9)$ than the average 0.13° in the serial (F)$_n$. For example, $r(1,2)$ is ($1.521 \pm 0.001) \times 10^{-10}$ m in both (F)$_n$ and (FDBO)$_n$ sequences; the values of $\theta(2,1,9)$ in (F)$_n$ and (FDBO)$_n$ are $102.72 \pm 0.02°$ and $102.77 \pm 0.08°$, respectively; $\Phi(17,16,12,13)$ is in the range $72.54°-72.78°$ in the serial (FDBO)$_n$. And it suggests that we can describe the basic structures of the polymers as their oligomers. Additionally, the optimized geometry parameters are in good agreement with X-ray data. The calculated $r(13,18)$ is 1.486×10^{-10} m in Table 1 with 1.489×10^{-10} m by X-ray in the monomer of FDBO, and the calculated $r(12,16)$ is 1.512×10^{-10} m with 1.497×10^{-10} m by X-ray. The calculated value $\theta(17,16,12)$ is $114.77°$ with the X-ray datum $114.29°$. The segments in bridge bond between two adjacent phenyls in the five-membered ring in these polymers are twisted so softly. They average in the oligomers 0.13° and 0.3° in $\Phi(2,3,4,9)$ to (F)$_n$ and (FDBO)$_n$, respectively. The structural feature of the seven-membered ring in (FDBO)$_n$ is the large dihedral angle $\Phi(12,13,18,19)$ (our calculated value is $42.14 \pm 0.4°$, which agrees with X-ray datum 43° quite well) because the dihedral angle between two phenyl rings in it is fixed by ring-bridged atoms which tend to keep their normal tetrahedral angles in their ring linkage to keep their conformational stability. Thus, the character of structure in the (FDBO)$_n$ is dramatically twisted in the seven-membered ring compared with PF, as seen in Figure 2. This characteristic of (FDBO)$_n$ will block
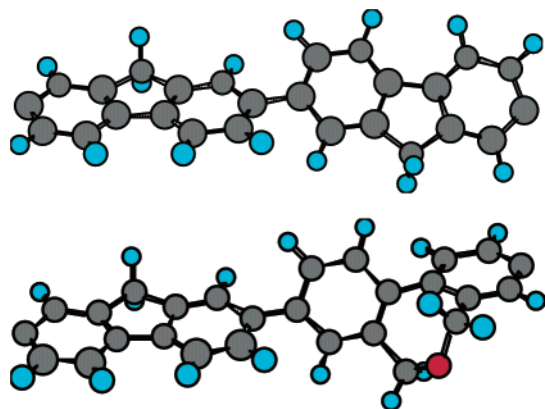
Figure 2. Torsion units of optimized structures for $(F)_8$ (top) and $(FDBO)_4$ (bottom).

the conjugation for conjugated backbone between the fluorene cells.

Front Molecular Orbitals. It will be useful to examine the highest occupied orbitals and the lowest virtual orbitals for these oligomers and polymers to provide the framework for the excited-state TD-DFT calculations in the subsequent section. We have found that the relative ordering of the occupied and virtual orbitals provides a reasonable qualitative indication of the excitation properties.[23] The HOMO orbitals and LUMO orbitals of the bifluorene $(F)_2$ and 2,7-fluorene-*alt-co*-5,7-dihydrodibenz[*c,e*]oxepin (FDBO) by B3LYP/6-31G are shown in Figure 3. Interestingly, the main characters of the front orbitals by HF/3-21G are the same as that by B3LYP/6-31G.

The HOMO and LUMO of both molecules are localized predominantly on the phenyl rings, as shown in Figure. For both $(F)_2$ and FDBO, there is antibonding between the bridge atoms and there is bonding between

the bridge carbon atom and its conjoint atoms in the same benzenes in the HOMO. On the contrary, there are bonding in the bridge single bond and the antibonding between the bridge atom and its neighbor in the same phenyl ring in the LUMO. The electronic cloud distributing in the front orbitals of FDBO is similar to that of $(F)_2$ on the fluorene ring. However, the electronic cloud in the benzene on the left side of the seven-membered ring is distributed less than that of other benzenes in FDBO. FDBO is bonding relaxation in the seven-membered ring compared with the fluorene ring from the electronic cloud picture. For the polymers, this implies the conjugation blocked in the seven-membered ring in PFDBO compared with PF.

Ionization Potentials and Electron Affinities. Additional information derived from our calculations provides insight into the interrelationship of structure and electronic behavior, in particular the response of the molecule to the formation of a hole or the addition of an electron. Table 2 contains the ionization potentials (IPs), electron affinities (EAs), both vertical (v; at the geometry of the neutral molecule) and adiabatic (a; optimized structure for both the neutral and charged molecule), and extraction potentials (HEP and EEP for the hole and electron, respectively) that refer to the geometry of the ions.[24,25]

To get the polymeric information, we extrapolate the linear to the infinite chain length. Figure 4 show plots of IPs, EAs, HEPs, EEPs, and SPE (h,e) as functions of reciprocal chain length for the oligomers studies, with assumed linear extrapolation to infinite chain length. All plotted data show excellent linearity (Figure 4). In all cases, the energy required to create a hole in the polymer is ~6 eV, while the extraction of an electron from the anion requires ~1.3 eV. We also synthesized the polymers by palladium-catalyzed Suzuki coupling
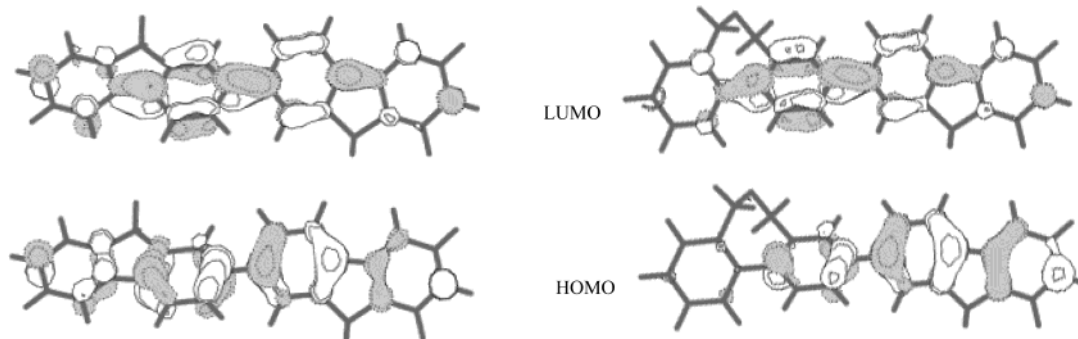

Figure 3. HOMO and LUMO orbitals of the $(F)_2$ (left) and FDBO (right).

Table 2. Ionization Potentials, Electron Affinities, Extraction Potentials, and "Small-Polaron" Stabilization Energies for Each Molecular (in eV)[a]

	IP(v)	IP(a)	HEP	EA(v)	EA(a)	EEP	SPE(h)	SPE(e)
$(F)_n$								
$n = 1$	7.53	1.76	1.89	0.98	0.83	−0.68	5.78	0.15
$n = 2$	6.64	6.51	6.51	0.07	−0.10	0.27	0.13	0.17
$n = 3$	6.27	6.16	6.06	−0.33	−0.46	0.60	0.11	0.13
$n = 4$	6.06	5.97	5.91	−0.54	−0.66	0.72	0.09	0.12
$n = 6$	5.80	5.75	5.81	−0.78	−0.87	0.95	0.04	0.09
$n = \infty$	5.37	5.39	5.40	−1.20	−1.24	1.27	0.02	0.04
$(FDBO)_n$								
$n = 1$	6.88	6.83	6.49	−0.05	−0.24	0.44	0.05	0.19
$n = 2$	6.33	6.24	6.15	−0.65	−0.80	0.94	0.08	0.15
$n = 3$	6.09	6.03	5.96	−0.91	−1.01	1.11	0.06	0.10
$n = 4$	5.95	5.91	5.86	−1.06	−1.15	1.24	0.04	0.09
$n = \infty$	5.58	5.59	5.57	−1.46	−1.49	1.52	0.01	0.03

[a] The suffixes (v) and (a) respectively indicate vertical and adiabatic values.
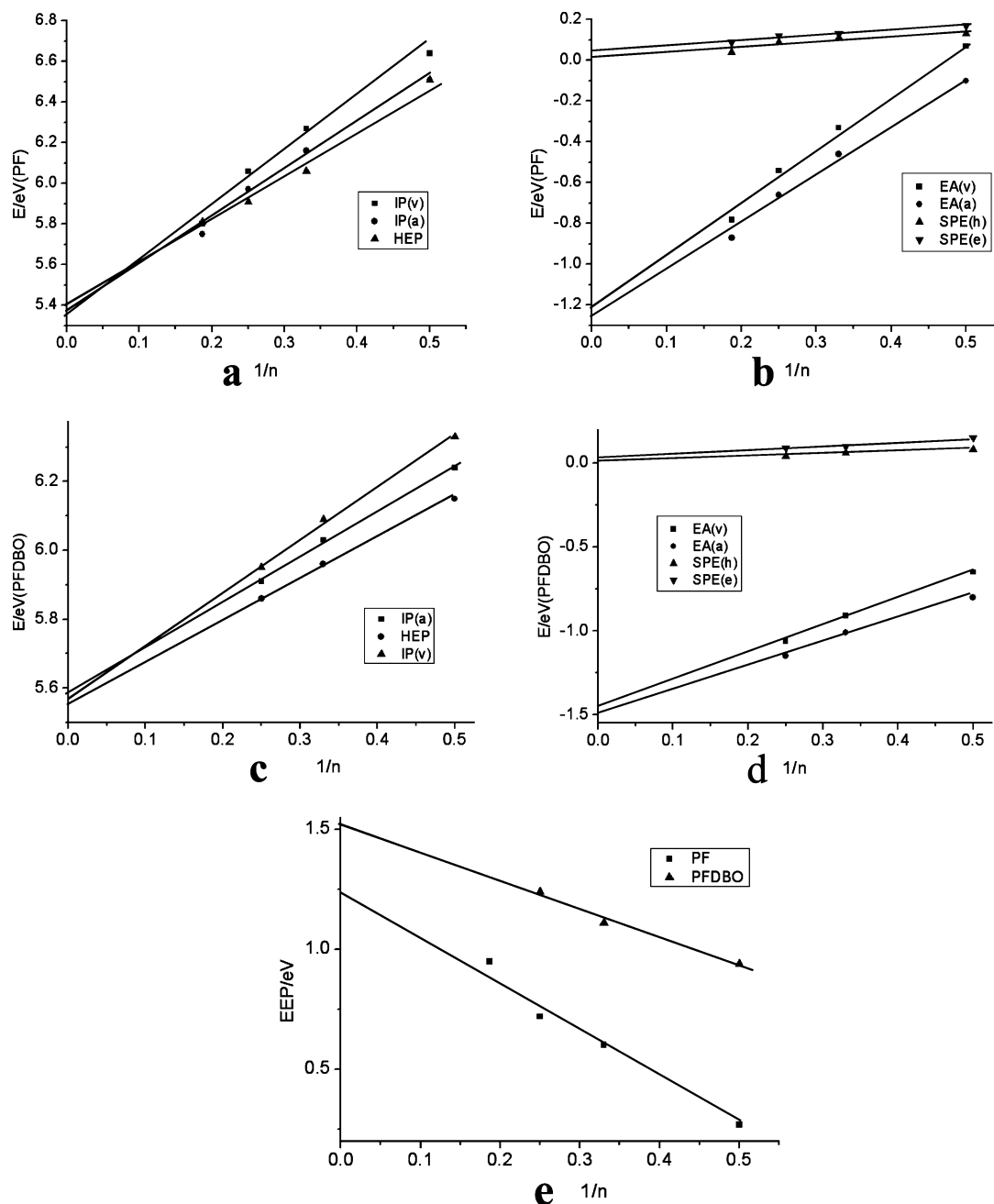
Figure 4. IP(v,a)s and HEP of PF (a), EA (v,a)s and SPE(h,e)s of PF (b), IP(v,a)s and HEP of PFDBO (c), EA(v,a)s and SPE(h,e)s of PFDBO (d), and EEPs of the two series (e) as a function of reciprocal chain length n in oligomers.

reaction and then got the correlative properties. Experimental values invariably refer to the solid state. For the IP(v), the measured values are 5.87 eV in both polymers. On the other hand, the electron affinity (the binding energy of the injected electron) cannot easily be obtained experimentally. The same calculations are also used to estimate self-trapping energies of positive and negative charges in the material. Indeed, the traps that characterize the electron transport in the material were identified as the states in which the injected electron is self-trapped in the individual molecules as a consequence of structural relaxation. The correct energy in our scheme is the energy gain of the excess electron due to structural relaxation, i.e., the difference EA(a) − EA(v), which we also report in Table 2 as the "small-polaron" stabilization energy (SPE) for the electron. Our value of 0.058 eV in polyfluorene is lower than

that in PFDBO. This suggests that the PFDBO appears to trap the electron more efficiently.
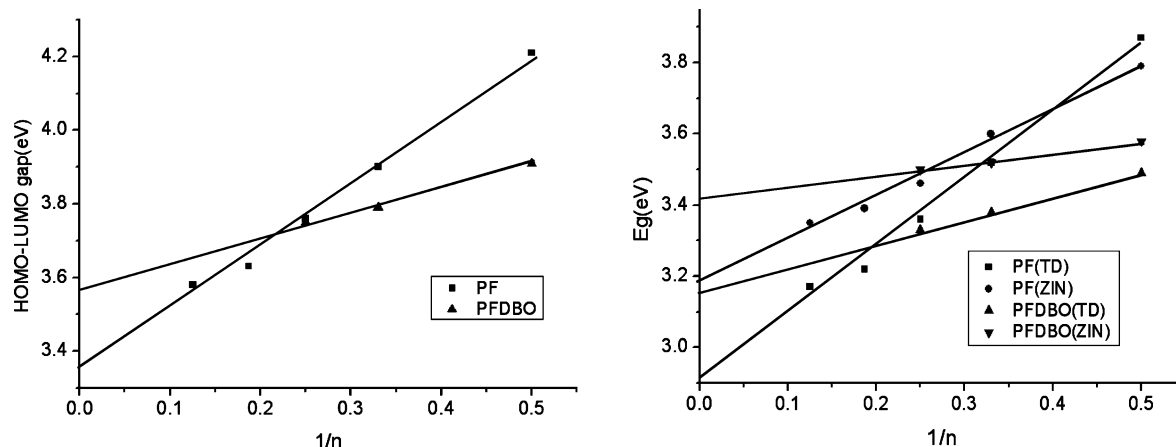
HOMO−LUMO Gaps and the Lowest Excitation Energies. It is well-known that the band gap of the polymer $(M)_n$ is the orbital energy difference between the highest occupied molecular orbital (HOMO) and the lowest unoccupied molecular orbital (LUMO),[26−28] when $n = \infty$. But it is difficult to obtain the correct data by experiment due to the experimental condition limit, such as interchain interactions, solvent effects, and so on. The experiment band gap is usually observed by two methods: the maximal wavelength in the spectra or the onset from CV-UV. They are valid when the lowest singlet excited state can be described by only one singly excited configuration in which an electron is promoted from HOMO to LUMO, and the experimental condition limit can be neglected. In our paper, the experimental

Table 3. HOMO−LUMO Gaps (eV) and the Lowest Excitation Energies (eV) of (F)$_n$ and (FDBO)$_n$

oligomer (F)$_n$	TD-DFT	ZINDO	Δ_{H-L}	oligomer (FDBO)$_n$	TD-DFT	ZINDO	Δ_{H-L}
$n = 1$	4.75	4.44	5.10	$n = 1$	3.96	4.20	4.31
$n = 2$	3.87	3.79	4.21	$n = 2$	3.49	3.58	3.91
$n = 3$	3.52	3.60	3.90	$n = 3$	3.38	3.52	3.79
$n = 4$	3.36	3.46	3.76	$n = 4$	3.33	3.50	3.75
$n = 6$	3.22	3.39	3.63	$E_g(n = \infty)$	3.15	3.42	3.58
$n = 8$	3.17	3.35	3.58	exptl	3.11[a]		
$E_g(n = \infty)$	2.91	3.18	3.33				
exptl	2.97[a]	2.88[b]					

[a] Our experimental band gap. [b] See ref 14.

Figure 5. HOMO−LUMO gaps (left) by B3LYP and the lowest excitation energies E_g (right) by ZINDO and TD-DFT as a function of reciprocal chain length n in oligomers of (F)$_n$ and (FDBO)$_n$.

data are obtained from the onset of CV-UV. Interestingly, in both series we studied here the maximal excitation is from HOMO to LUMO. Our HOMO−LUMO gaps are obtained from density functional theory (DFT) calculations. To compare with the experiment data, we also calculate the lowest excitation energies of the oligomers to extrapolate the band gap. Time-dependent DFT (TD-DFT) and ZINDO calculations were employed to examine the low-lying singlet excited states of the oligomers. The HOMO−LUMO gaps Δ_{H-L}, the lowest excitation energies E_g of the oligomers, and the extrapolated band gaps of PF and PFDBO are presented in Table 3. The experimental band gaps which acquired from cyclic voltammograms of their films modified platinum electrodes in MECN, and they are located in the last line to compare with the calculated data. There is a good linear relation between the HOMO−LUMO gap, the lowest excitation energies, and the inverse chain length (see Figure 5).

In the plot, we can extrapolate the HOMO−LUMO gaps to the infinite chain length to get 3.33 and 3.58 eV to PF and PFDBO, respectively. The band gaps from Δ_{H-L} are close to the experiment data, 2.97 eV to PF and 3.11 eV to PFDBO. Their deviations are no more than 0.5 eV. Therefore, it is desirable to obtain the useful information in the nature of the lowest singlet excited state by employing the HOMO−LUMO gap.[29] Because the HOMO−LUMO gap is easy to get, the approach can also be used to provide valuable information on estimate band gaps of oligomers and polymers, especially treating even larger systems.[30−32] However, the orbital energy difference between HOMO and LUMO is still an approximate estimate to the transition energy since the transition energy also contains significant contributions from some two-electron integrals. The real situation is that an accurate description of the

lowest singlet excited state requires a linear combination of a number of excited configurations.

To get some useful information for the experiment of the band gaps, we turn to the spectrum methods. All the cases of our studies here, a long-wavelength transition with large oscillator strength (>0.7) was obtained, implying a strong transition. Good agreement is found between the observed E_g values and the calculated by both methods, which obtained by extrapolating the resultant linear relationship to infinite chain length, and the TD-DFT method is better compared to the ZINDO's in meeting the experimental data. From Table 3, one can see that the TD-DFT predictions systematically underestimate the band gaps of those polymers, with the average deviation of about 0.05 eV. Furthermore, for the PF, there is more than the experiment datum from the ref 14 by only 0.03 eV, while the results of ZINDO deviate about 0.27 eV. Three factors may be responsible for the error. One is that calculations on a few longer oligomers may be required so that more data could be used in linear regression. Another is that the predicted band gaps are for isolated gas-phase chains, while experimental band gaps are measured in the condensed phase where interchain interactions may be significant.[12,33,34] Additionally, the methods of calculation and experiment have fault in themselves. However, our TD-DFT calculations suggest a relatively large band gap of 3.15 eV for PFDBO, 0.24 eV broader than the predicted band gap of PF, 2.91 eV.

Despite the good agreement between the calculated excitation energies and the experimental data, it is also necessary to check the validity of these excitation energies which are calculated by TD-DFT. The excitation energies calculated by TD-DFT with the current exchange-correlation functions are not reliable when the calculated excitation energies are higher than the

Table 4. TD-DFT Excitation Energies (eV) and the Negative of HOMO Energies ($-\epsilon_{HOMO}$) (eV) of Oglimers (F)$_n$ and (FDBO)$_n$

| oligomer (F)$_n$	TD-DFT	$-\epsilon_{HOMO}$	oligomer (FDBO)$_n$	TD-DFT	$-\epsilon_{HOMO}$
$n = 1$	4.75	5.80	$n = 1$	3.96	5.48
$n = 2$	3.87	5.38	$n = 2$	3.49	5.44
$n = 3$	3.52	5.24	$n = 3$	3.38	5.40
$n = 4$	3.36	5.17	$n = 4$	3.33	5.39
$n = 6$	3.22	5.12			
$n = 8$	3.17	5.09			

negative of the HOMO energies.[17] The negative of HOMO energies ($-\epsilon_{HOMO}$) and the TD-DFT excitation energies are displayed in Table 4. In Table 4, it shows that in all cases the TD-DFT excitation energies are below the negative of HOMO energies and thus may be numerically reliable. However, the band gaps extrapolated by TD-DFT are better compared with the HOMO−LUMO gaps when the experimental data are taken into consideration. The deviations are 0.06 and 0.05 eV for PF and PFDBO by TD-DFT, while that of HOMO−LUMO gaps are 0.36 and 0.47 eV for PF and PFDBO, respectively. TD-DFT with the B3LYP functional is expected to be a relatively reliable tool for evaluating the excitation energies of low-lying excited states for small- and medium-sized molecules. Otherwise, unlike TD-DFT computationally expensive and difficult to treat even larger systems, the advantage of the HOMO−LUMO gap is the simple approach. So it is always used to estimate the band gaps of large molecules. In all cases, the band gaps extrapolated by not only the lowest excitation energies (E_gs) but also the HOMO−LUMO gaps (Δ_{H-L}s) have the same trend to meet the experimental data. On all accounts, the results of each method indicate the same conclusion that the decreasing of the conjugation in the backbone of PFDBO broadens its band gap.

In addition, the effective conjugation length (ECL) can be estimated from calculations on a series of oligomers. The effective conjugation length is the repeat unit number at which saturation of a property occurs. The information on the effective conjugation length of the polymers is very useful to the synthetic strategies.[28,35] It will estimated for all selected oligomers based on the convergence of the calculated excited energy of the first dipole-allowed excited state with increasing chain length. We take 0.01 eV as the convergence threshold of the excitation energies with the chain length, based on the obtained linearity between the excitation energy and reciprocal chain length.[17] So the ECL of PF is estimated at around 14 units. For PFDBO, a slightly shorter ECL at about 8 units is estimated by TD-DFT. By ZINDO, they are 11 and 6 units to PFDBO and PF, respectively. Both methods come out the same result that PFDBO has a shorter effective conjugation length than PF because the dramatically twisted segment in the structure of PFDBO blocks the conjugated backbone.

Absorption Spectra. On the basis of the optimized geometry, we calculated the absorption spectrum of these oligomers in Table 5. Interestingly, we found there is a quite well linearity between the macroabsorption and the reciprocal chain length seen in Figure 6. Thus, we list the extrapolating data to $1/n = 0.0$ in the last but one line in Table 5. The results agree well with those from experiment.

Though the λ_{abs} by ZINDO is shorter than that by TD-DFT to the same molecule, they have the same trend of
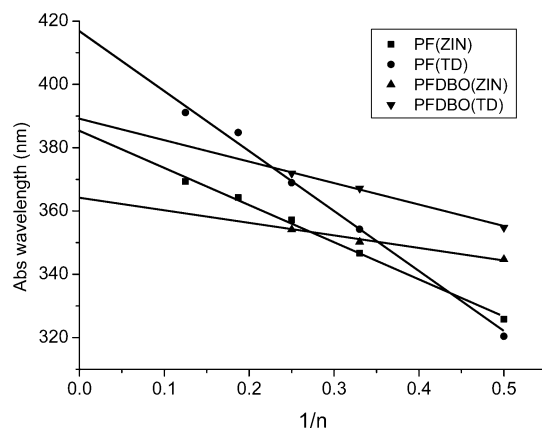

Figure 6. Absorption wavelengths by ZINDO and TD-DFT as a function of $1/n$ in oligomers.
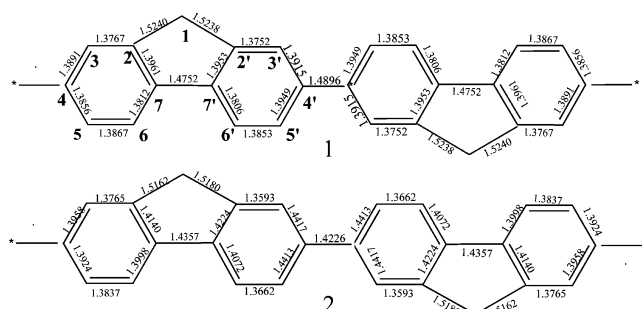
Figure 7. Comparison of the excited structure (**2**) with the ground (**1**) of (F)$_2$.

Table 5. Absorption Wavelengths (λ_{abs} in nm) Computed at the ZINDO and TD-DFT Methods

	(F)$_n$			(FDBO)$_n$	
n	ZINDO	TD-DFT	n	ZINDO	TD-DFT
1	247.9	260.8	1	293.8	313.2
2	325.8	320.4	2	344.7	354.8
3	346.7	354.2	3	350.2	367.2
4	357.1	368.9	4	354.1	371.9 (355.5)
6	364.2	384.8	∞(polymer)	363.1	389.5
8	369.3	391.1 (349.4)	exptl	353	
∞(polymer)	385.1	417.2			
exptl	383				

increasing with chain length adding. Our values of 385.1 and 363.1 nm for PF and PFDBO, respectively, by ZINDO are close to the experimental data. The λ_{abs} calculated by TD-DFT is slightly longer than the experimental data by 35.2 and 34.5 nm for PF and PFDBO. The difference is 30 nm between PF and PFDBO by experiment, and our values match it quite well that there are 22 nm by ZINDO and 27 nm by TD-DFT. However, the results of the both methods show that PFDBO has shorter maximal absorption wavelength than PF.

Properties of Excited Structures and Emission Spectra. In Figure 7 we can see the excited structure of the bifluorene (**2**) by CIS/3-21G compared with its ground structure (**1**) by HF/3-21G, in view of the valid comparison.

The optimized results showed both ground and excited structures of the bifluorene had C_2 point group symmetry. All the bond lengths of the left benzene are longer in the excited state than in the ground state by $(0.01-0.002) \times 10^{10}$ m, except $r(2,3)$ is shortened by
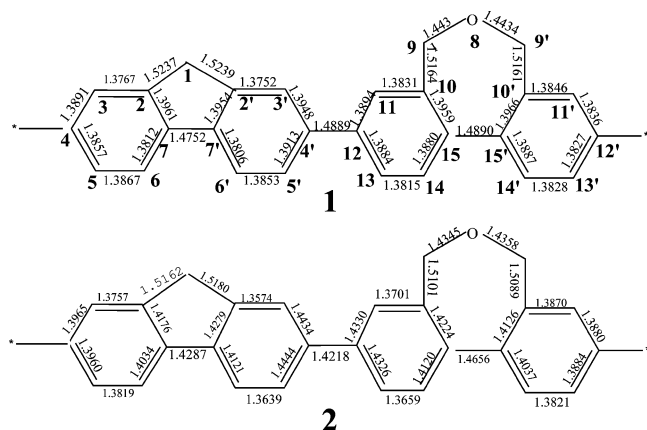
Figure 8. Comparison of the excited structure (**2**) with the ground (**1**) of FDBO.

0.0002×10^{10} m. While the bond lengths of the right benzene are longer by about 0.035×10^{10} m except $r(5',6')$ and $r(2',3')$ shorter than its ground state by about 0.02×10^{10} m, the single bond between the fluorene units shortened by 0.067×10^{10} m than its ground state. The bridge single bond between two benzene $r(7',7)$ is shorter than the ground state by 0.0395×10^{10} m. The dihedral angle $\Phi(2,7,7',2')$ broadens from $-0.045°$ to $0.092°$; that is, the $r(7,7')$ rotates during exciting. And the single bond between the two fluorene units also rotated after excitation. The dihedral angle of the two adjacent fluorene units shortened from $36.62°$ to $6.49°$. There is strong coplanar tendency of fluorine ring with neighboring aromatic ring in the excited state.

The structure of excited monomer of PFDBO by CIS/3-21G compares with its ground-state structure by HF/3-21G in Figure 8. All the single bonds in the five-membered ring and the seven-membered ring shortened after being excited, while the double bond lengths of these rings increased in the excited state. The single bond length $r(7,7')$ shortened by 0.0465×10^{10} m and $r(1,2)$ by 0.0075×10^{10} m compared with the ground state, and $r(4',12)$ shortened by 0.0671×10^{10} m because

of excitation. The bridge bonds between two conjugation segments rotate to some extent. The dihedral angle $\Phi(2,7,7',2')$ reduced from $0.14°$ to $0.09°$, $\Phi(3',4',12,13)$ from $36.0°$ to $7.8°$, and $\Phi(10,15,15',10')$ from $42.7°$ to $39.1°$. It is obvious that the excited structure has a strong coplanar tendency in both the series; that is, the conjugation is better in the excited structure. For $(F)_2$, the dihedral angles are no larger than $8°$ in the excited state. However, there is still large dihedral angle in the seven-membered ring of FDBO, $39.1°$, which reduced only $3.5°$ after being excited. It indicates that the conjugation for conjugated backbone interdicted in the rigid twisted seven-membered ring of PFDBO. The larger band gap and the shorter wavelength in the spectra in PFDBO result from this structural character to a certainty. The changes of the structures during the excitation can be prefigured from the characters of front orbitals. Comparing Figure 7 and Figure 8 with Figure 3, we can see that the structure will be tight when the antibonding changes into bonding, i.e., the bond length $r(7,7')$, $r(5,6)$, $r(5',6')$, $r(2,3)$, and $r(2'3')$ in both molecules and $r(4',12)$, $r(10,11)$, $r(13,14)$, and $r(15,15')$ in FDBO shortened after excitation where are nodes in the HOMO and bonding in the LUMO. Contrarily, the bond length will increase when the bonding changes into antibonding. This can be seen from the bond lengths $r(2,7)$, $r(2',7')$, $r(6,7)$, $r(6',7')$, $r(3,4)$, $r(3',4')$, $r(4,5)$, and $r(4',5')$ in both systems and $r(12,13)$ and $r(14,15)$ in FDBO increasing in the excitation compared with the ground state.

The same result can be seen in maximal emission wavelengths of the oligomers in Table 6. The experimental data of the polymers are listed in the last line in order to be compared, and the spectrum is shown in Figure 9. Their excited geometries are optimized by ab intio CIS and the wavelengths computed by ZINDO and TD-DFT. We select the dimer and quatermer of PF parallelism to monomer and dimer of PFDBO, in view of the molecular weight.

As shown in Table 6, the values of the emission wavelengths of the oligomers reflect the same as the

Table 6. Emission Wavelengths (λ_{emi} in nm and cm^{-1} in Parentheses) Computed at the ZINDO and TD-DFT Methods

	$(F)_n$			$(FDBO)_n$	
n	ZINDO	TD-DFT	n	ZINDO	TD-DFT
2	374.4 (26 709)	374.3 (26 717)	1	340.7 (29 353)	366.1 (27 314)
4	410.5 (24 360)	433.5 (23 068)	2	398.6 (25 086)	415.9 (24 044)
exptl	417 (23 980), 436 (22 935)[a]			397 (25 188), 414 (24 154) sh[b]	

[a] An approximate peak in the spectrum. [b] A shoulder peak.
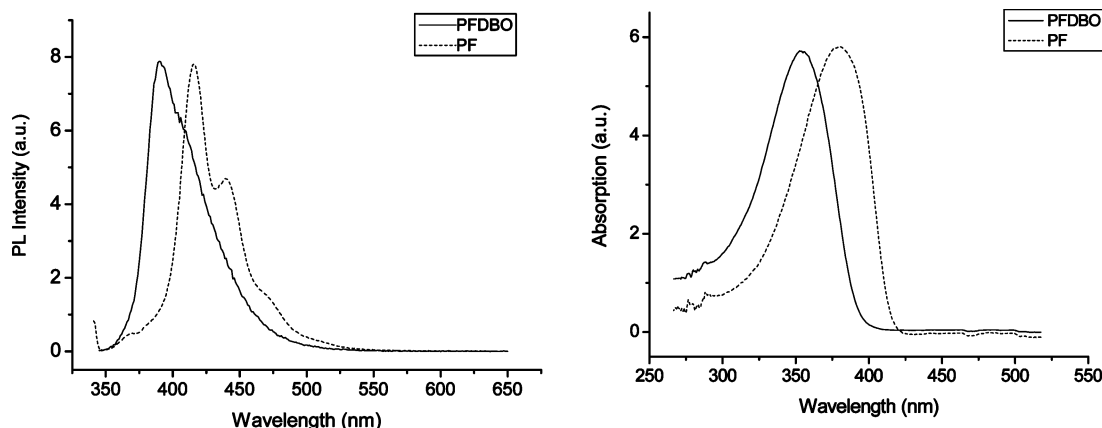
Figure 9. PL (left) and absorption (right) spectra of the polymers by experiment (in THF at room temperature).

absorption wavelengths. The oligomeric λ_{emi} of $(FDBO)_n$ is shorter than that of $(F)_n$ by the range 8.2−33.3 nm. It is easy to see that our values are close to the experimental data (20 or 39 nm) from the table. Comparing Table 5 to Table 6, the stocks of the oligomers by ZINDO in both series are about 50 nm, while the values computed by TD-DFT are in the range 53−65 nm. The results of both methods are in accord with the experimental data (the difference is 34 or 54 nm) very well. Furthermore, the emission wavelengths of the oligomers of $(FDBO)_n$ are shorter than that of the counterparts of $(F)_n$. It shows again the effect on the properties by the twist segment in the structure of PFDBO.

4. Conclusion

The chain length dependence of IPs, EAs, and Δ_{H-L} was studied employing the density functional theory with B3LYP functional, while λ_{abs} and E_gs of oligomers of the both sequences using ZINDO and the time-dependent density functional theory. Our polymeric values from extrapolation, not only the IPs and EAs but also the E_gs and λ_{abs} of the oligomers, are in good linearity. The extrapolation results of E_gs and λ_{abs} are in good agreement with the experimental data. On all accounts, the rigid twist in the structure of PFDBO result in the conjugation decreasing, and it is easy to add an electron and to ionize compared with PF. To the importance, it results in a broader band gap and shorter maximal absorption and emission wavelengths in the spectra for PFDBO than PF.

Supporting Information Available: Syntheses of 3,9-dibromo-5,7-dihydrodibenz[c,e]oxepin and poly[(9,9-dihexyl-2,7-fluorene-alt-co-5,7-dihydrodibenz[d,f][1,3]oxepin and optimized oligomer structures of PF and PFDBO. This material is available free of charge via the Internet at http://pubs.acs.org.

References and Notes

(1) Horst, W.; Susanne, S.; Stefan, J.; Alexander, V. U.; Axel, H. E. M. *Macromolecules* **2003**, *36*, 3374−3379.
(2) Mushrush, M.; Facchetti, A.; Lefenfeld, M.; Katz, H. E.; Marks, T. J. *J. Am. Chem. Soc.* **2003**, *125*, 9414−9423.
(3) Bredas, J. L.; Silbey, R.; Boudreaux, D. S.; Chance, R. R. *J. Am. Chem. Soc.* **1983**, *105*, 6555−6559.
(4) Tavan, P.; Schulten, K. *J. Chem. Phys.* **1986**, *85*, 6602−6609.
(5) Beljonne, D.; Shuai, Z.; Cornil, J.; dos Santos, D. A.; Bredas, J. L. *J. Chem. Phys.* **1999**, *32*, 267−276.
(6) Lahti, P. M.; Obrzut, J.; Karasz, F. E. *Macromolecules* **1987**, *20*, 2023−2026.
(7) Burrows, H. D.; Seixas de Melo, J.; Serpa, C.; Arnaut, L. G.; Miguel, N. da G.; Monkman, A. P.; Hamblett, I.; Navaratnam, S. *J. Chem. Phys.* **2002**, *285*, 3−11.
(8) Scheinert, S.; Schliefke, W. *Synth. Met.* **2003**, *139*, 501−509.
(9) Yamamoto, T.; Fujiwara, Y.; Fukumoto, H.; Nakamura, Y.; Koshihara, S. Y.; Ishikawa, T. *Polymer* **2003**, *44*, 4487−4490.
(10) Morisaki, Y.; Ishida, T.; Chujo, Y. *Polym. J.* **2003**, *35*, 501−506.
(11) Yang, N. C.; Chang, S.; Suh, D. H. *Polymer* **2003**, *44*, 2143−2148.
(12) Winokur, M. J.; Slinker, J.; Huber, D. L. *Phys. Rev. B* **2003**, *67*, 184106.
(13) Anne, D. B.; Isabelle, L.; Ye, T.; Marie, D.; Serge, B.; Pierre, B.; Maxime, R.; Jimmy, B.; Mario, L. *Chem. Mater.* **2000**, *12*, 1931−1936.
(14) Zeng, G.; Yu, W. L.; Chua, S. J.; Huang, W. *Macromolecules* **2002**, *35*, 6907−6914.
(15) Lee, S. H.; Nakamura, T.; Tsutsui, T. *Org. Lett.* **2001**, *3*, 2005−2007.
(16) Wong, K. T.; Wang, C. F.; Chou, C. H.; Su, Y. O.; Lee, G. H.; Peng, S. M. *Org. Lett.* **2002**, *4*, 4439−4442.
(17) Ma, J.; Li, S. H.; Jiang, Y.-S. *Macromolecules* **2002**, *35*, 1109−1115.
(18) Klaerner, G.; Miller, R. D. *Macromolecules* **1998**, *31*, 2007−2009.
(19) Sheats, J. R.; Antoniadis, H.; Hueschen, M.; Leonard, W.; Niller, H.; Moon, R.; Roitman, D.; Stocking, A. *Science* **1996**, *273*, 884−888.
(20) Wohlgenannt, M.; Tandon, K.; Mazumdar, S.; Ramasesha, S.; Vardeny, Z. V. *Lett. Nature* **2001**, *409*, 494−498.
(21) Burrows, P. E.; Shen, Z.; Bulovic, V.; McCarty, D. M.; Forrest, S. R.; Cronin, J. A.; Thompson, M. E. *J. Appl. Phys.* **1996**, *79*, 7991−8006.
(22) Rathore, R.; Abdelwahed, S. H.; Guzei, I. A. *J. Am. Chem. Soc.* **2003**, *125*, 8712−8713.
(23) De Oliveira, M. A.; Duarte, H. A.; Pernaut, J.-M.; De Almeida, W. B. *J. Phys. Chem. A* **2000**, *104*, 8256−8262.
(24) Curioni, A.; Andreoni, W. *IBM J. Res. Dev.* **2001**, *45*, 101−113.
(25) Curioni, A.; Boero, M.; Andreoni, W. *Chem. Phys. Lett.* **1998**, *294*, 263−271.
(26) Hay, J. P. *J. Phys. Chem. A* **2002**, *106*, 1634−1641.
(27) Curioni, A.; Andreoni, W.; Treusch, R.; Himpsel, F. J.; Haskal, E.; Seidler, P.; Heske, C.; Kakar, S.; van Buuren, T.; Terminello, L. *J. Appl. Phys. Lett.* **1998**, *72*, 1575−1577.
(28) Hong, S. Y.; Kim, D. Y.; Kim, C. Y.; Hoffmann, R. *Macromolecules* **2001**, *34*, 6474−6481.
(29) Belletete, M.; Beaupre, S.; Bouchard, J.; Blondin, P.; Leclerc, M.; Durocher, G. *J. Phys. Chem. B* **2000**, *104*, 9118−9125.
(30) Rogero, C.; Pascual, J. I.; Gomez-Herrero, J.; Baro, A. M. *J. Chem. Phys.* **2002**, *116*, 832−836.
(31) Wang, J. L.; Wang, G. H.; Zhao, J. J. *Phys. Rev. B* **2001**, *64*, 205411.
(32) Cabrera-Trujillo, J. M.; Robles, J. *Phys. Rev. B* **2001**, *64*, 165408.
(33) Wang, I.; Estelle, B. A.; Olivier, S.; Alain, I.; Baldeck, P. L. *J. Opt. A: Pure Appl. Opt.* **2002**, *4*, S258−S260.
(34) Wu, C.; Liu, T. L.; Hung, W. Y.; Lin, Y. T.; Wong, R. T.; Chen, Y. M.; Chien, Y. Y. *J. Am. Chem. Soc.* **2003**, *125*, 3710−3711.
(35) Menzel, H.; Mowery, M. D.; Cai, M.; Evans, C. E. *J. Phys. Chem. B* **1998**, *102*, 9550−9556.